Advances in Differential Equations and Control Processes 2026, 33(3), 4510.
doi: https://doi.org/10.59400/adecp4510

Article

Nonlinear hybrid impedance control for hydrodynamically coupled dual-arm underwater manipulators

Sandeep Yadav[1,*], Sunil Kumar[1], Manoj Goyal[1], Pravin Kumar[2]

[1] Department of Mechanical Engineering, Sant Longowal Institute of Engineering and Technology (SLIET), Longowal 148106, India; sunillumar@sliet.ac.in (SK); manojgoyal@sliet.ac.in (MG)

[2] Department of Metallurgical Engineering and Materials Science (MEMS), Indian Institute of Technology Indore (IIT Indore), Indore 453552, India; Phd2301205004@iiti.ac.in

* **Corresponding authors:** Sandeep Yadav, sandeepyadav@sliet.ac.in

CITATION

Yadav S, Kumar S, Goyal M, et al. Nonlinear hybrid impedance control for hydrodynamically coupled dual-arm underwater manipulators. Advances in Differential Equations and Control Processes. 2026; 33(3): 4510. https://doi.org/10.59400/adecp4510

ARTICLE INFO

Received: 15 June 2026
Revised: 16 August 2026
Accepted: 20 August 2026
Available online: 31 August 2026

Abstract: Underwater robotic manipulators require precise force–position interaction control to perform reliable operations in uncertain and dynamically coupled underwater environments. However, the performance of conventional impedance controllers is significantly degraded by nonlinear hydrodynamic disturbances, structural flexibility, and dynamic coupling effects. This paper proposes a hydrodynamic coupling-aware hybrid impedance control framework for a dual-arm with two-link underwater robotic manipulator (DT–URM). The proposed strategy integrates a passive impedance formulation with a compensation gain and a proportional–integral–derivative (PID)-bas–ed auxiliary loop to enhance interaction stability, trajectory-tracking accuracy, and disturbance-rejection capability. A DT–URM model is developed in SolidWorks and validated in MATLAB/Simulink under nonlinear underwater operating conditions. To evaluate controller robustness under realistic dynamics, the framework is further extended to a flexible two-link underwater manipulator by incorporating hydrodynamic and buoyancy effects into the system model. In addition, interaction constraints are introduced to maintain safe distances from virtual boundaries during manipulation tasks. Comparative simulation results demonstrate that the proposed controller reduces trajectory tracking and force-tracking errors by 18.5%, respectively, compared with conventional impedance control. Furthermore, disturbance rejection capability and settling time are improved by 19%, respectively, while maintaining stable operation under varying environmental conditions. The results confirm that the proposed control framework improves dynamic interaction performance and robustness, making it suitable for underwater inspection, maintenance, and cooperative manipulation applications.

Keywords: dual-arm underwater robotic manipulator; hydrodynamic coupling; impedance control; force–position control; PID controller; MATLAB/Simulink simulation; hydrodynamic modelling

1. Introduction

Interaction between robotic arms and their surroundings is crucial for autonomous underwater tasks to succeed. In underwater jobs such as welding, inspection, and repair, the robotic arm's end effector must either contact a surface or maintain a specific distance from it [1]. These tasks are tricky because they involve dealing with complex underwater conditions. Underwater robotic arms must adapt to these conditions and handle forces during operation. To accomplish these tasks accurately and keep the system stable, a control plan that can manage both the arm's position and the force between the end part and the environment is needed. The robotic arm and its end-effector must work well together to achieve this. They must effectively respond to conditions. The manipulator end-effector and the environment must be controlled properly. This is necessary for task execution.

Robots need to be able to control the force they use when they interact with things around them. This is especially true when they interact with surfaces. People have come up with ways to make robots do this. Some of these ways are control and direct force control [1,2]. There are also force and position control, parallel force and position control, and impedance control. Impedance control is very useful because it helps the robot work well with its surroundings. It does this by setting up a relationship between the force exerted by the robot and how it moves. This means the robot can work safely and smoothly when it must touch things [3,4]. The foundational work by Song et al., Heshmati-Alamdari et al., and Tabatabaee-Nasab and Moosavian introduced impedance-based formulations for analysing static and dynamic interactions between manipulators and their environments, including bond graph representations of system dynamics [5–7].

Subsequent studies have expanded the application of impedance control to various robotic systems. In particular, Liu et al. [8] investigated interaction control in legged robots by employing bond graph modelling and vision/force sensing to regulate the driving-point impedance and improve environmental interaction performance. Passive actuation strategies have also been explored to achieve stable and dissipative contact interactions in uncertain environments [9]. Yao et al. [10] proposed multiple impedance control (MIC) for coordinated force/position tracking in free-flying space manipulators. In practical scenarios involving frictional contact, velocity–force relationships have been utilised to estimate surface characteristics [11]. It has been investigated how stable force regulation is when using a combination of PI-based force control and PD-based position control. This was tested when the robotic arm works in environments that give a bit. The force regulation stability was checked using a PI-based force controller and a PD-based position controller. This happens when the manipulator operates in an environment [12].

In underwater robotics, impedance control has been applied to underwater vehicle–manipulator systems (UVMs), demonstrating improved interaction performance in simulation studies [13]. External force control strategies that avoid explicit dynamic compensation have also been proposed for UVMs [14, 15]. For dual-arm systems, multiple impedance control (MIC) and augmented object model (AOM) approaches achieve improved tracking accuracy and effective collision response. Robust impedance-based force tracking methods capable of handling environmental uncertainties have been developed by Dongming et al., Farivarnejad and Moosavian [16, 17]. Furthermore, Mishra and Vaz [18] introduced a bond graph-based impedance control framework incorporating a passive foundation concept; however, the use of a linear controller limits disturbance rejection capability and steady-state accuracy in complex environments.

Despite these advancements, existing approaches often neglect the combined effects of hydrodynamic disturbances, structural flexibility, and coupled dynamics in underwater manipulators. In particular, the application of hybrid impedance control frameworks to flexible, dual-arm underwater systems remains limited [19].

This study addresses the limitations of existing impedance control strategies by showing a way to control a special robot arm that can move underwater. The new method is based on an idea that was discussed before in some studies [19,20]. **Figure 1** shows the robot arm has two links that can bend, which makes it useful for working underwater. The proposed approach integrates a proportional–integral–derivative (PID) controller into the impedance loop to enhance stability, improve tracking performance, and eliminate steady-state errors in the presence of environmental disturbances [21, 22]. The system is modeled using bond graph techniques, with flexible links represented as Euler beams discretised into multiple segments, and the end-effector incorporating the mass of a manipulator [23]. The control framework is implemented and validated through simulation using the SYMBOLS Sonata software [24,25]. The results demonstrate effective force–position regulation and stable interaction during underwater manipulation, confirming the suitability of the proposed method for complex contact-based operations. The remainder of this paper is organized as follows. Section 2 presents the hybrid impedance control formulation. Section 3 describes the system modeling and controller implementation. Section 4 presents the simulation setup, while Section 5 discusses the simulation results and performance evaluation.

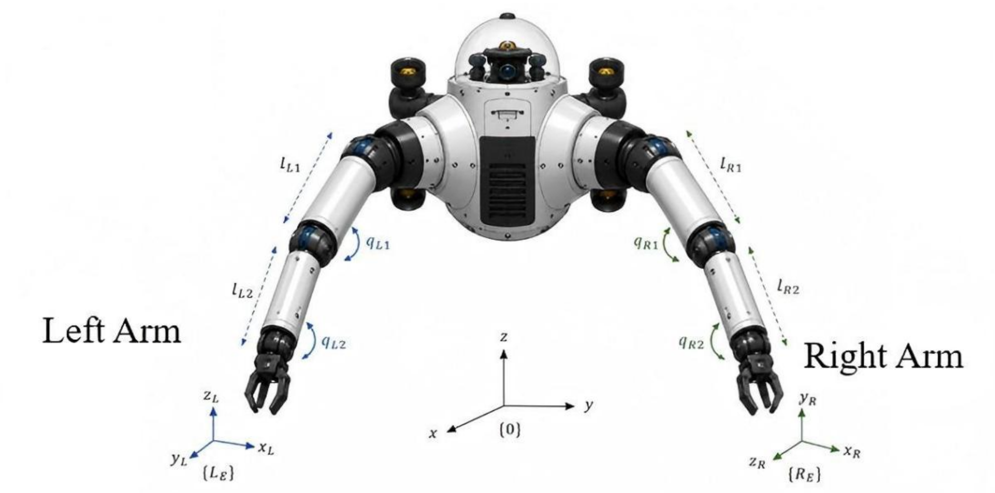

Figure 1. Dual-arm underwater robot manipulator.

Novelty

Unlike conventional impedance controllers, the proposed framework integrates impedance regulation with PID-based dynamic compensation to improve interaction stability, trajectory tracking accuracy, and disturbance rejection under nonlinear hydrodynamic conditions. In addition, the controller is evaluated using a coupled simulation framework incorporating SolidWorks, MATLAB/Simulink, Simscape Multibody, and bond graph modeling to represent rigid-body dynamics, structural flexibility, and underwater environmental interactions. Comparative simulations demonstrate consistent improvements over conventional impedance control under identical operating conditions.

2. Methodology and model integration

The proposed methodology uses a hierarchical modelling and simulation framework for the dual-arm underwater robotic manipulator. First, the SolidWorks model is developed to define the manipulator geometry, link dimensions, joints, mass properties and assembly configuration. These parameters are then used in MATLAB/Simulink for nonlinear dynamic modelling, trajectory generation, PID tuning and implementation of the proposed hybrid impedance controller.

A two-link flexible manipulator model is used as a reduced-order representation for analysing hydrodynamic effects, structural flexibility and the bond-graph-based impedance formulation. The corresponding bond graph/Symbols Sonata model is used for energy-flow and impedance analysis of the controller.

For system-level validation, a three-link model is implemented in Simscape Multibody within MATLAB/Simulink to represent rigid-body dynamics, joints and multibody motion. The controller receives position/velocity feedback from the model and generates the required actuator commands.

Thus, each tool has a specific role: SolidWorks-geometric modelling; MATLAB/Simulink-dynamic modelling and control; two-link model-reduced-order controller analysis; bond graph/Symbols Sonata -impedance and energy-flow analysis; and three-link Simscape model-multibody-level controller validation. This integrated framework enables consistent evaluation of trajectory tracking, force regulation and disturbance rejection.

The methodology begins with the development of a 3D model of the DT–URM using SolidWorks, followed by dynamic modeling in MATLAB/Simulink, considering inertia, buoyancy, hydrodynamic drag, Coriolis forces, and environmental disturbances. PID controllers are initially implemented for joint trajectory tracking, and controller gains are optimized using the integral of time multiplied by absolute error (ITAE) criterion. Subsequently, Cartesian-space impedance control is applied to regulate the interaction between the manipulator end-effector and the underwater environment. The impedance controller establishes the desired dynamic relationship between position and contact force.

3. Control formulation & system dynamics

Building upon the dynamic formulation and control framework described in the previous section, the design of the interaction controller is now presented with a focus on achieving compliant and stable force–position regulation. Given the presence of nonlinear hydrodynamic effects, structural flexibility, and environmental uncertainties, a control strategy capable of explicitly regulating the force–motion relationship is required. Impedance control provides a suitable framework for this purpose, as it enables the specification of desired dynamic behaviour at the end-effector during contact tasks [26]. However, conventional impedance control approaches may exhibit performance limitations under persistent disturbances and modeling uncertainties.

To overcome these challenges, a hybrid impedance control strategy is adopted in this work, integrating a passive foundation concept with a PID-based compensation mechanism [27,28]. This combination enhances disturbance rejection, improves steady-state accuracy, and ensures stable interaction under varying operating conditions [29]. Equation (1) presents the formulation of the impedance controller, along with its implementation using bond graph modeling for the underwater robotic manipulator system.

$$M_d(\ddot{x} - \ddot{x}_d) + B_d(\dot{x} - \dot{x}_d) + K_d(x - x_d) = F_e \tag{1}$$

where M_d, B_d, and K_d denote the desired inertia, damping, and stiffness matrices, respectively, and F_e represents the interaction force. The proposed control framework is evaluated in MATLAB/Simulink based on trajectory tracking accuracy, force regulation, settling time, overshoot, and disturbance rejection performance under underwater operating conditions.

3.1. Dynamic model

The dynamics of the dual-arm with two-link underwater robotic manipulator are represented by Equation (2) written below

$$M(q)q^{\cdot\cdot} + C(q, q^{\cdot})q^{\cdot} + D(q^{\cdot}) + G(q) + Fh + Fe = \tau \tag{2}$$

The dual-arm with two-link underwater robotic manipulator dynamics describe the relationship between the joint motion, applied torques, and underwater forces. The model considers the effects of inertia, Coriolis and centrifugal forces, hydrodynamic damping, gravity, buoyancy, added mass, and environmental interaction for the applied joint torque is expressed in Equation (3). The total inertia includes rigid-body and added-mass contributions,

$$M = MRB + MA. \tag{3}$$

3.2. Conventional impedance control

The conventional impedance controller establishes the desired relationship between the end-effector position error and the interaction force. The task-space impedance relationship is expressed in Equation (4).

$$Mde^{\cdot\cdot} + Bde^{\cdot} + Kde = Fe - Fd, \tag{4}$$

Conventional impedance control establishes a desired dynamic relationship between the end-effector position error and the interaction force. It regulates the manipulator's motion while allowing compliant interaction with the underwater environment.

3.3. Proposed hybrid impedance control

To improve trajectory tracking and disturbance rejection, a PID compensation term is incorporated into the conventional impedance control. The proposed control input is expressed in Equation (5).

$$\tau = \tau_{IC} + \tau_{PID} + \tau_H \tag{5}$$

where is τ_{IC} the conventional impedance-control component, τ_{PID} provides position-error compensation, and τ_H represents the additional hybrid/nonlinear compensation term. The PID compensation term is given by Equation (6).

$$\tau_{PID} = K_{Pe} + KI + K_{De} \tag{6}$$

The proposed formulation combines force regulation and position tracking while maintaining compliant interaction with the underwater environment.

3.4. PID tuning

The PID gains are optimized using the integral of time multiplied by absolute error (ITAE) criterion, as given in Equation (7).

$$ITAE = \int_0^T t \mid e(t) \mid dt \tag{7}$$

where T denotes the simulation time. The optimized gains are subsequently used in the proposed hybrid impedance controller. The same operating conditions, reference trajectories, initial conditions, and performance criteria are maintained for comparison with the conventional impedance controller.

4. Impedance controller

Impedance is defined as the dynamic relationship between force (effort) and velocity (flow) in a mechanical system. In underwater robotic manipulators, accurate force–position interaction is difficult because of nonlinear hydrodynamic effects, structural flexibility, environmental disturbances, and parameter uncertainties. These factors degrade tracking accuracy and interaction stability during underwater operations.

To overcome these limitations, a hybrid impedance control framework is proposed to control a dual-arm robot designed for underwater operation. **Figure 2** illustrates the mechanical configuration of the one-DOF manipulator with a passive foundation, while the corresponding bond graph representation of the hybrid impedance control module is presented in **Figure 3**. The proposed controller combines impedance regulation with PID-based compensation through a passive foundation structure and a PID-based compensation controller. The PID controller improves trajectory tracking, compensates for disturbances, and enhances the overall dynamic response of the manipulator.

In the bond graph representation (**Figure 3**), M_p, R_p, and K_p denote the mass, damping, and stiffness parameters of the passive foundation, respectively. The base mass is represented by M_b, while m_p denotes the lumped mass of the manipulator link. The reference excitation angular velocity $f_{v,ref}$ is generated by the actuator system in **Figure 1** and applied to drive the manipulator motion.

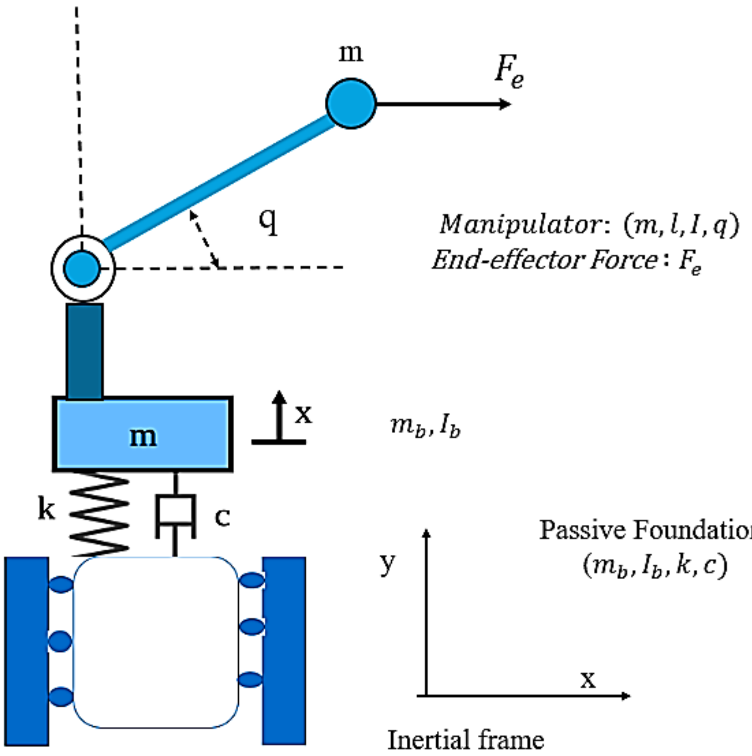

Figure 2. Schematic representation of the one-DOF robotic manipulator with a passive foundation.

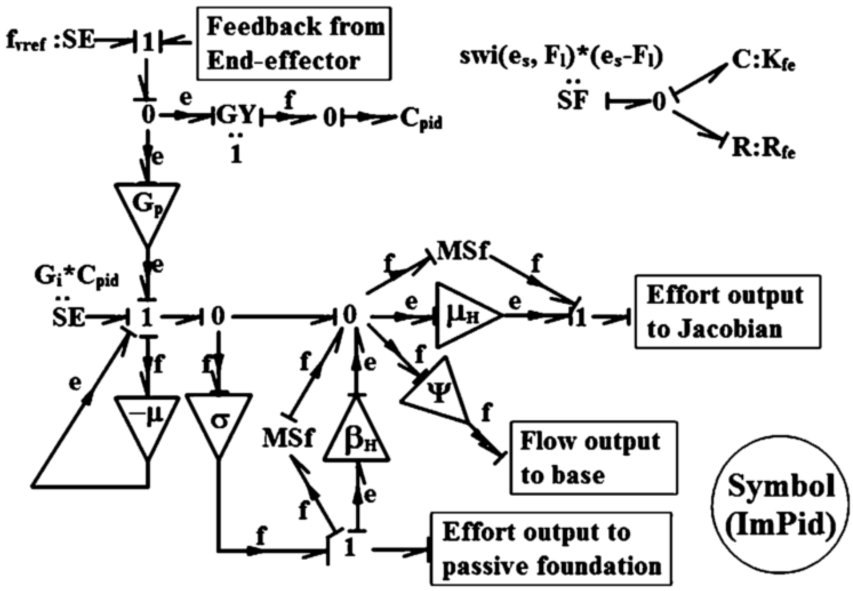

Figure 3. Bond graph representation of the proposed hybrid impedance control module.

The bond graph model in **Figure 3** consists of two parts that work together: the physical part and the controller part. The physical part concerns the manipulator's base and links and how it interacts with the surrounding water. The controller part has things like the foundation that does not need power to work, a controller that changes how the system reacts, and a way to fix the movement so it is more stable. The foundation that does not need power helps control the forces that are at work by changing how the system reacts to these forces. This helps balance the control of forces and the movement of the manipulator when it is doing tasks, with the bond graph model. The bond graph model is essential for underwater manipulator operation.

The proposed control strategy enhances robustness against parameter variations and ensures bounded tracking errors through high feed-forward gains and feedback compensation. The transfer function relating robotic tip flow to environmental effort is derived from the signal-flow representation of the bond graph model presented in **Figure 3**, following the methodology reported by Pathak and Mukherjee.

This system is based on how the manipulator moves and how it reacts to forces. The proposed controller enables compliant interaction between the manipulator and its environment. Therefore, impedance control is employed to regulate the interaction. Impedance is the relationship between the force the underwater manipulator feels and how fast its end is moving. This relationship characterises how the underwater manipulator will react when it touches something in the water. The impedance control scheme is used to make sure the underwater manipulator behaves correctly. For underwater robotic manipulators, this relationship is significantly influenced by nonlinear dynamics, hydrodynamic disturbances, and system uncertainties, leading to variations in force and position during operation.

High-precision trajectory tracking often results in increased apparent impedance, which can adversely affect interaction performance by amplifying contact forces and reducing compliance, particularly under wake-induced disturbances. Therefore, an appropriate impedance control strategy is required to balance trajectory tracking, interaction stability, and robustness against uncertainties in a two-link flexible underwater robotic manipulator.

The system response is evaluated by establishing the relationship by finding the connection between the flow at the tip of the robot and the effort from the environment. This connection is found using a graph that shows how signals flow, which is based on a model called a bond graph. This is done by following the steps that are explained in some papers [18, 23]. The resulting formulation provides a basis for evaluating interaction behavior and controller performance under varying operating conditions.

4.1. Simulation setup

The proposed control framework is evaluated through numerical simulations carried out in the MATLAB/Simulink environment, incorporating multibody dynamics using Simscape Multibody (Sim-Mechanics). A three-link robotic manipulator model is developed to represent the kinematic and dynamic behavior of the system under underwater operating conditions. Underwater robotic manipulators are critical.

The end-effector interaction with the environment is modeled as contact with a moving planar surface, enabling the assessment of force–position regulation under dynamic interaction scenarios. The transformation of interaction forces between task space and joint space is achieved using a Jacobian-based formulation, allowing accurate mapping of forces and velocities within the control loop.

To capture realistic system behaviour, damping and compliance effects are incorporated through appropriate matrices, representing both structural flexibility and environmental interaction characteristics. These parameters are selected to reflect the influence of hydrodynamic disturbances and contact dynamics on the manipulator performance.

For a fair comparison, both the conventional impedance controller and the proposed hybrid impedance controller were evaluated using the identical simulation environment. The manipulator geometry, hydrodynamic coefficients, desired trajectory, environmental stiffness, damping parameters, external disturbance profile, simulation duration (5 s), solver settings, and sampling time were kept unchanged. Only the controller architecture differed, thereby ensuring that the observed performance improvements resulted solely from the proposed control strategy.

4.2. Impedance control implementation using MATLAB/Simulink

The impedance control was put in place so that the manipulator end-effector and the underwater environment around it could work together smoothly. This control strategy makes sure that the force on the end-effector is just right for its movement. The impedance control strategy regulates the force on the manipulator end-effector based on how it's moving, which means it sets a desired behavior for the manipulator end-effector. This means that the impedance control creates a relationship between the force on the manipulator end-effector and how it moves, and this relationship can be written down in a mathematical formula is given bellow in Equation (8):

$$w^E = K_v t_e \tag{8}$$

where w^E denotes the end-effector wrench, t_e represents the end-effector twist, and K_v is the velocity gain matrix. By controlling the impedance rather than only the position, the manipulator can effectively absorb impact loads and maintain stable interaction with moving objects or environmental constraints.

The impedance control structure developed in MATLAB/Simulink is illustrated in **Figure 4**. The controller utilizes both pose and twist feedback to generate the corrective joint torques required for trajectory tracking and force regulation. The commanded torque is expressed as Equation (9):

$$\tau_{qv} = J^T[K_p\,(q_d - q) + K_v(t_d - t_e)] \tag{9}$$

where J is the manipulator Jacobian matrix, K_p and K_v are the position and velocity gain matrices, respectively. The terms $(q_d - q)$ and $(t_d - t_e)$ represent the pose and twist errors between the desired and actual end-effector states. The desired pose trajectory q_d and desired twist trajectory t_d are supplied to the controller, and the resulting torque command is computed from the corresponding tracking errors.

To model the interaction with the environment, compliance K_{Fq} and K_{Ft}, were incorporated to transform the environmental position and velocity into equivalent end-effector references. The orientation of the end-effector was maintained through additional feedback loops that regulate orientation errors, ensuring stable operation during contact tasks. Consequently, the overall actuator torque applied to the manipulator can be expressed in Equation (10) as

$$\tau = \tau_{qv} - \tau_v - \tau_E - \tau_g \tag{10}$$

where τ_v, τ_E, and τ_g represent the velocity-dependent torque, environmental interaction torque, and gravity/buoyancy compensation torque, respectively.

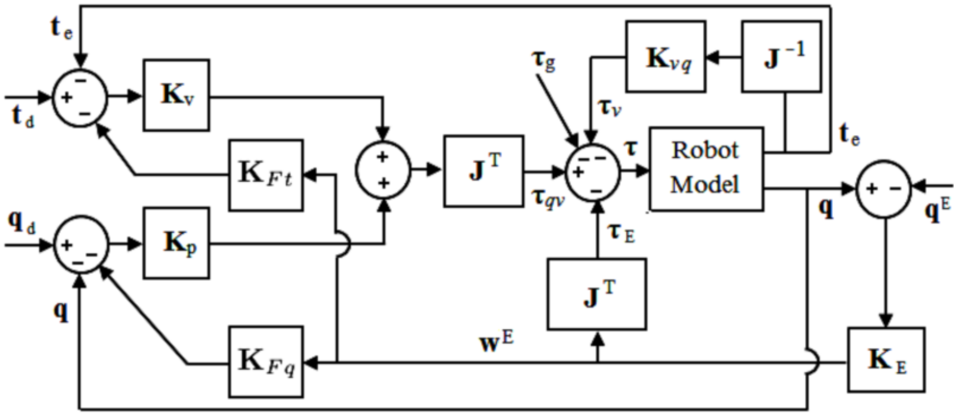

Figure 4. Block diagram of the impedance control model.

The Jacobian transformation required for converting task-space control forces into joint-space torques was implemented through a dedicated Simulink subsystem, as shown in **Figure 5**.

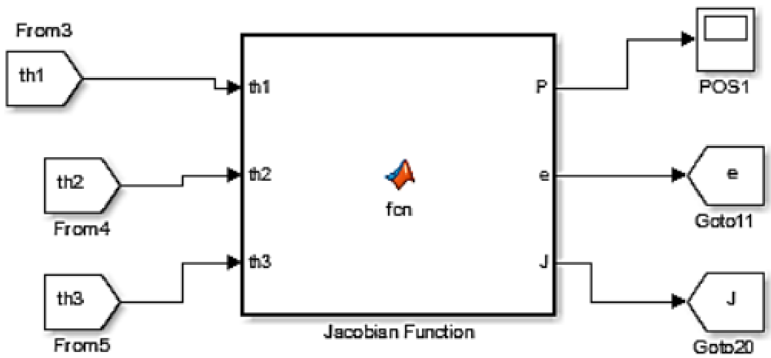

Figure 5. Jacobian function Simulink model for impedance control.

4.3. Jacobian transformation

The Jacobian matrix is employed to map the end-effector velocity in task space to the corresponding joint velocities and torques of the underwater robot manipulator. In the proposed impedance control framework, the end-effector velocity is measured and fed back to the controller for generating the required corrective torque commands. This transformation enables the conversion of task-space force commands into joint-space actuation torques.

The kinematic relations describing in Equations (11) and (12) the end-effector motion in the (Z)- and (Y)-directions are given by

$$Z_{tip2} = Z_{cm} + r\cos\beta + L(\cos(\beta_1) + \cos(\beta_{12})) \tag{11}$$

$$Y_{tip2} = Y_{cm} + r\sin\beta + L(\sin(\beta_1) + \sin(\beta_{12})) \tag{12}$$

here,

$$\beta_1 = \beta + \theta_1 \text{ and } \beta_{12} = \beta + \theta_1 + \theta_2.$$

represent the angular positions of the first and second links, respectively.

By differentiating Equations (5) and (6), the Jacobian matrix relating the end-effector velocity to the joint velocities can be obtained as Equation (13)

$$\begin{matrix} Z_{tip2} \\ Y_{tip2} \end{matrix} = L \begin{bmatrix} -\sin(\beta_1) - \sin(\beta_{12}) & -\sin(\beta_{12}) \\ \cos(\beta_1) + \cos(\beta_{12}) & \cos(\beta_{12}) \end{bmatrix} \begin{bmatrix} \dot{\theta}_1 \\ \dot{\theta}_2 \end{bmatrix} \tag{13}$$

The Jacobian matrix was implemented in MATLAB/Simulink using dedicated transformation blocks. The corresponding Jacobian subsystem is shown in **Figure 5** and Equation (14), where the transformation coefficients are defined as

$$\begin{gathered} \mu_1 = -L\sin(\beta_1) - \sin(\beta_{12}), \mu_2 = -L(\cos(\beta_1) + \cos(\beta_{12})), \\ \mu_3 = -L\sin(\beta_{12})), \text{and } \mu_4 = -L\cos(\beta_{12})) \end{gathered} \tag{14}$$

These coefficients are used to transform the task-space velocity and force information into equivalent joint-space quantities required by the impedance controller.

Figure 5 illustrates the MATLAB/Simulink implementation of the Jacobian subsystem employed in the proposed control framework.

Furthermore, the impedance force-control subsystem responsible for generating compliant interaction forces is presented in **Figure 6**. The complete impedance-control implementation for the robotic manipulator, integrating trajectory generation, Jacobian transformation, force regulation, and manipulator dynamics, is illustrated in **Figure 7**.

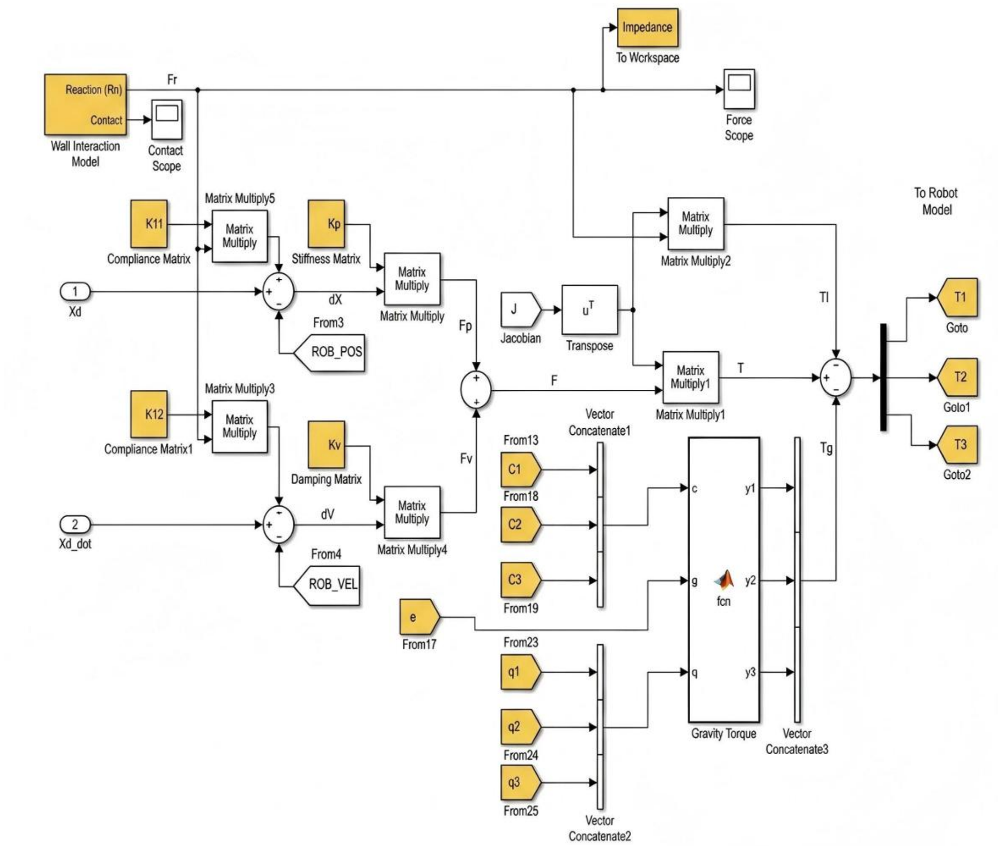

Figure 6. Impedance force control Simulink model subsystem of **Figure 7**.

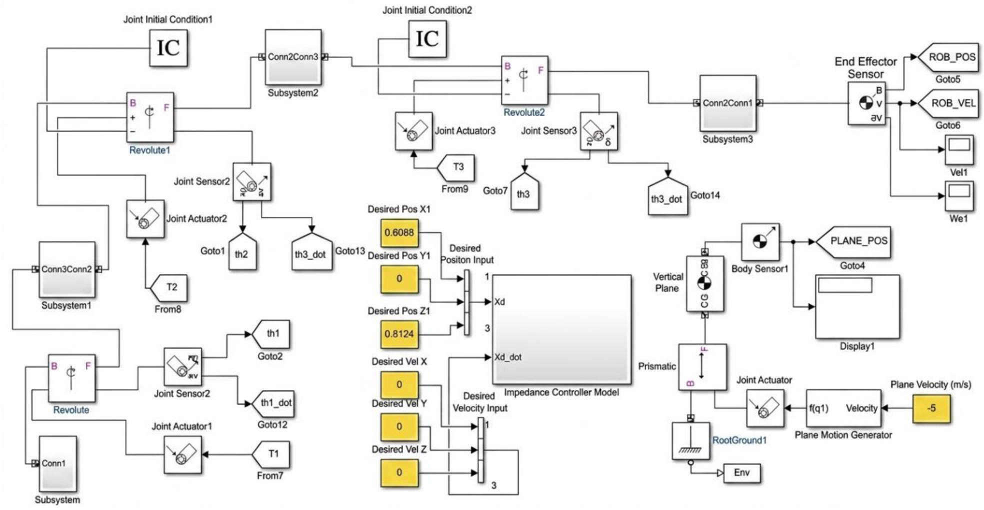

Figure 7. Impedance control Simulink model for four-link robotic manipulator.

The controller parameters employed in the simulation study were selected as matrices in Equations (15) and (16)

$$K_p = \begin{bmatrix} 15 & 0 & 0 \\ 0 & 0 & 0 \\ 0 & 0 & 0 \end{bmatrix} K_v = \begin{bmatrix} 200 & 0 & 0 \\ 0 & 200 & 0 \\ 0 & 0 & 200 \end{bmatrix} \tag{15}$$

$$K_{Fq} = \begin{bmatrix} 0.02 & 0 & 0 \\ 0 & 1 & 0 \\ 0 & 0 & 1 \end{bmatrix} K_{Ft} = \begin{bmatrix} 0.01 & 0 & 0 \\ 0 & 1 & 0 \\ 0 & 0 & 1 \end{bmatrix} \tag{16}$$

The proposed control strategy was tested to see how well it works when things are moving around. A flat surface was moved at a speed of −0.2 m per second in the simulation. The results show that the impedance controller does what it is supposed to do. It controls the forces that are at work when the surface and the controller interact. At the time, the impedance controller makes sure that the surface follows the path it is supposed to follow. The controller is also very good at dealing with problems. This means it can work well and reliably when it is used underwater to manipulate things, when the environment around it is changing.

5. Results and discussion

The dual–two–link underwater robot manipulator was tested with a method of controlling it. This new way was checked using computer simulations that were very close to what happens in the water. The computer model included things that happen in the water, like buoyancy and drag. The robot had to follow a path while touching a surface that was moving and tilted. The results of the simulation showed that this new way of controlling the dual–two–link underwater robot manipulator worked well. It controlled the force of the robot on the surface. Made sure the robot moved smoothly along the path. The dual–two–link underwater robot manipulator was able to do this when there were big waves and other things happening in the water that could affect it. The new control strategy helped the dual–two–link underwater robot manipulator work correctly. The objective was to investigate the controller's capability in achieving accurate trajectory tracking, compliant environmental interaction, force regulation, and disturbance rejection during underwater manipulation tasks.

Figure 8 illustrates the contact interaction process of the DT–URM under the proposed control framework. During the initial stage, the end-effector follows the prescribed trajectory in free space without environmental contact. As contact is established, the impedance controller regulates the interaction force through compliant motion, reducing impact effects and preventing excessive contact forces. Subsequently, stable contact is maintained while the manipulator adapts its motion to follow the environmental surface. The smooth transition between free-space motion and constrained interaction demonstrates the effectiveness of the proposed controller in achieving compliant underwater manipulation.

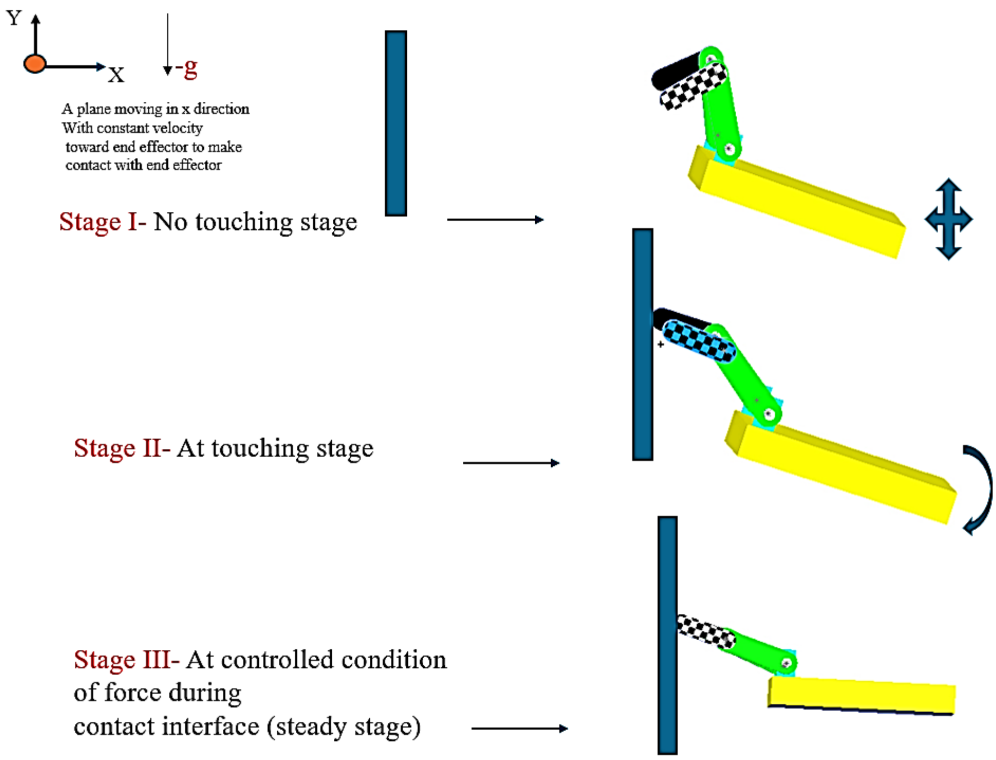

Figure 8. Contact interaction process of the manipulator under the impedance control model of DT–URM.

The corresponding contact-state response is presented in **Figure 9**. The manipulator initially operates in a non-contact state before short-duration contact events occur during the approach phase. Continuous contact is established after approximately 0.5 s and remains stable throughout the simulation period. The absence of repeated contact losses indicates that the controller successfully maintains force-regulated interaction under varying environmental conditions.

The force response of both manipulator arms is shown in **Figure 10**. Transient force peaks are observed during the initial impact and re-contact phases; however, these disturbances are rapidly attenuated by the controller. The force responses of both arms converge smoothly toward the desired reference force, demonstrating coordinated dual-arm operation and balanced force distribution. To further evaluate force regulation performance, **Figure 11** compares the desired and actual force responses. The actual force closely follows the desired force throughout the simulation, with a maximum force-tracking error of less than 1 N and an overall tracking accuracy of approximately 98–99%. The smooth response and absence of significant oscillations confirm the effectiveness of the proposed controller in maintaining stable environmental interaction.

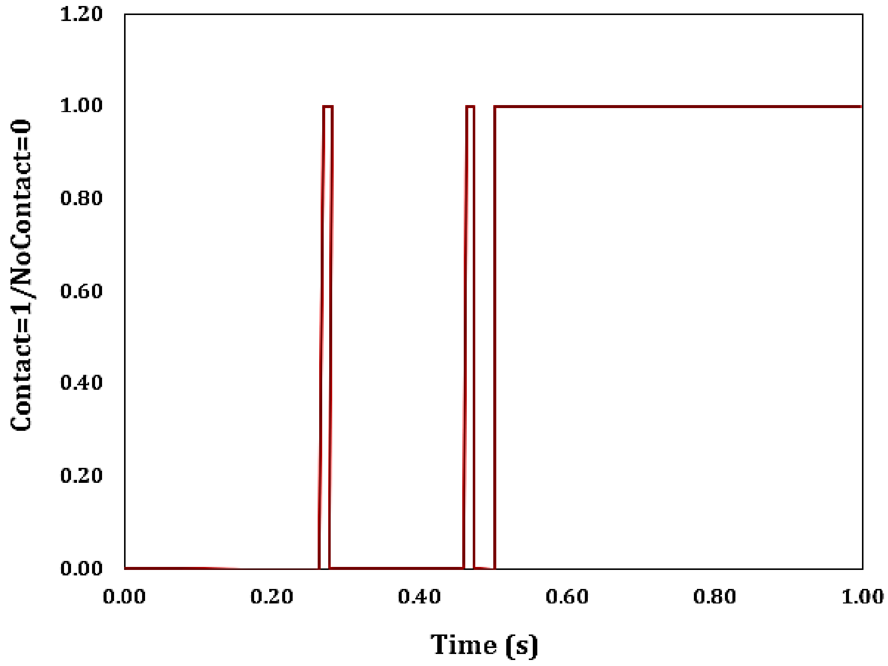

Figure 9. Contact and no-contact duration with time.

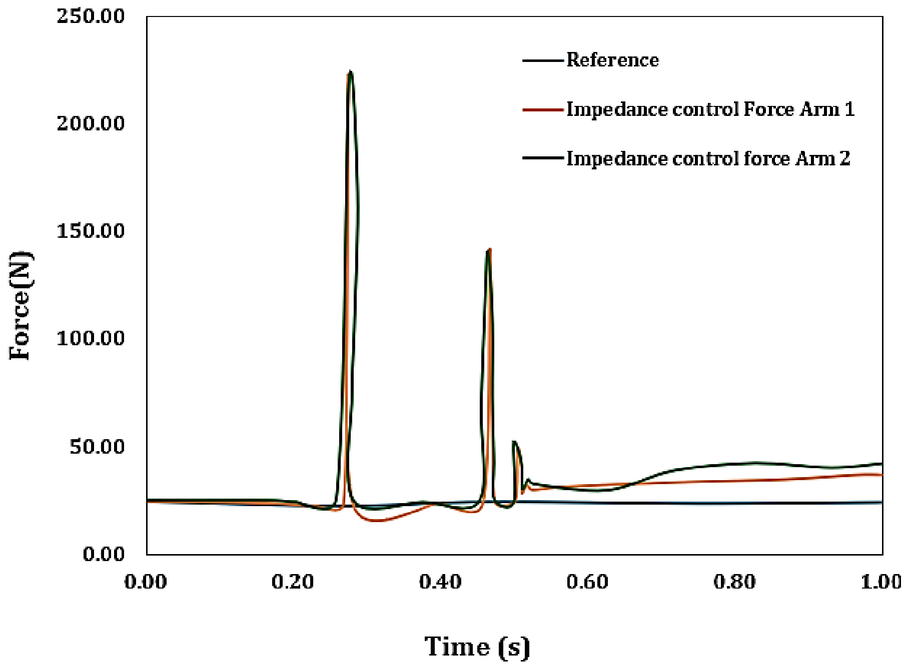

Figure 10. Force responses of the left and right manipulator arms under the proposed hybrid impedance controller.

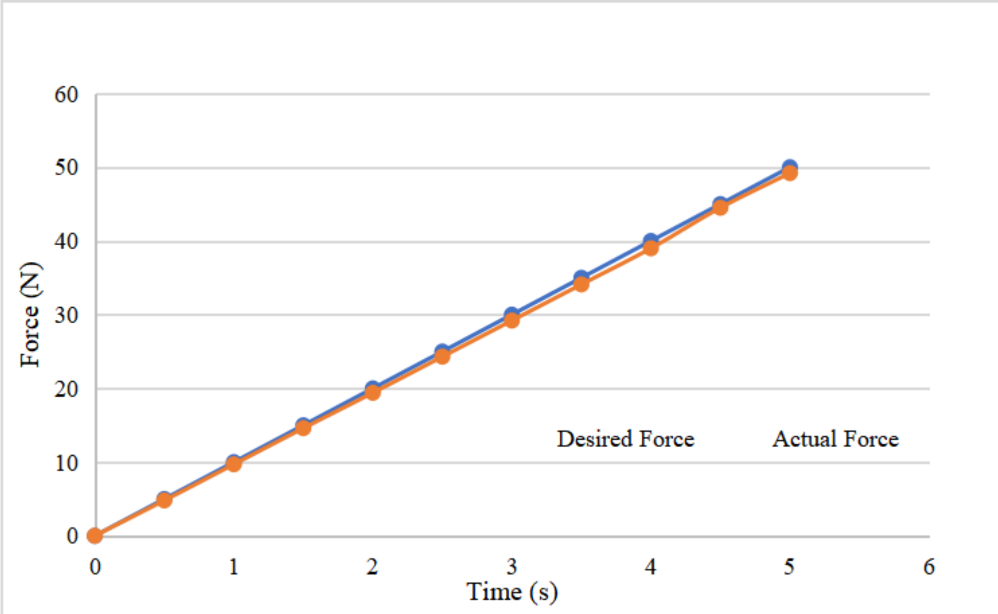

Figure 11. Comparison of desired and actual forces for force-tracking error analysis.

The end-effector position responses shown in **Figure 12** demonstrate accurate trajectory-tracking performance during environmental interaction. The position components remain smooth and bounded throughout the simulation period. While the lateral and vertical positions remain nearly constant, the motion along the primary tracking direction follows the desired trajectory without significant deviation. The absence of abrupt position fluctuations confirms the stability of the proposed control strategy.

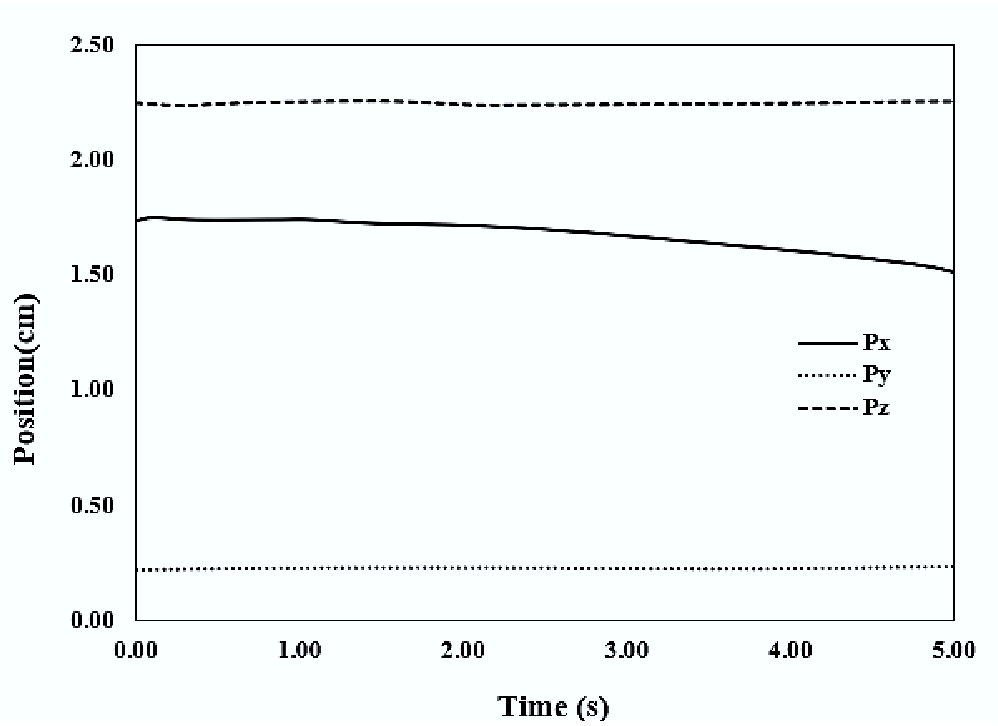

Figure 12. End-effector Cartesian position response (in the X, Y, and Z directions) under the proposed hybrid impedance controller.

The velocity responses presented in **Figures 13** and **14** provide further insight into the dynamic behavior of the manipulator. Following contact establishment, transient oscillations appear due to impact forces and hydrodynamic disturbances. However, the damping action introduced by the hybrid impedance controller rapidly suppresses these oscillations, resulting in smooth and stable velocity profiles. The derivative component of the PID compensation plays a significant role in reducing vibration amplitudes and improving transient stability. Consequently, the controller effectively minimizes the influence of flexible-link dynamics and underwater disturbances.

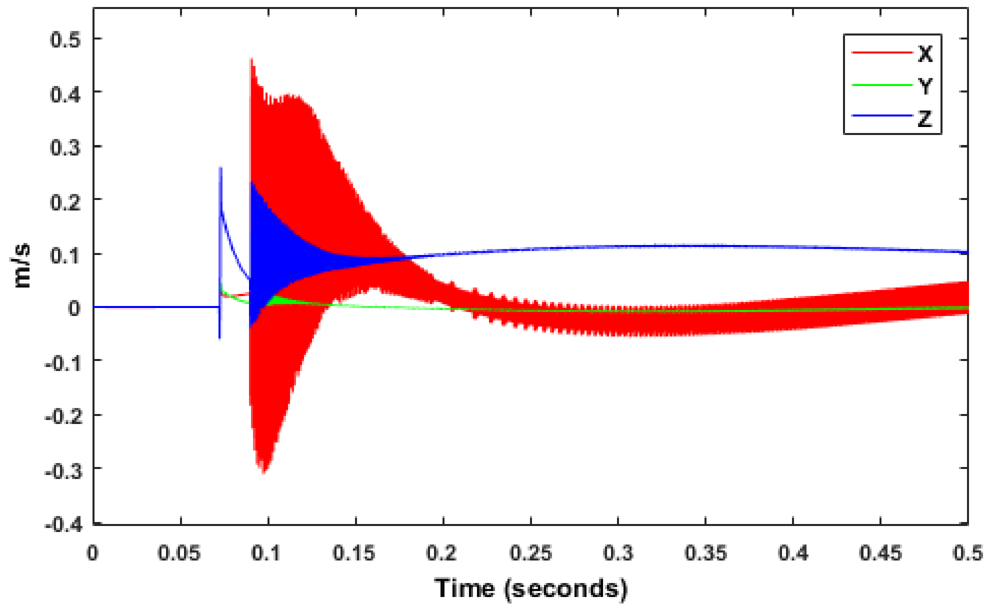

Figure 13. End-effector linear velocity response in the X, Y, and Z directions.

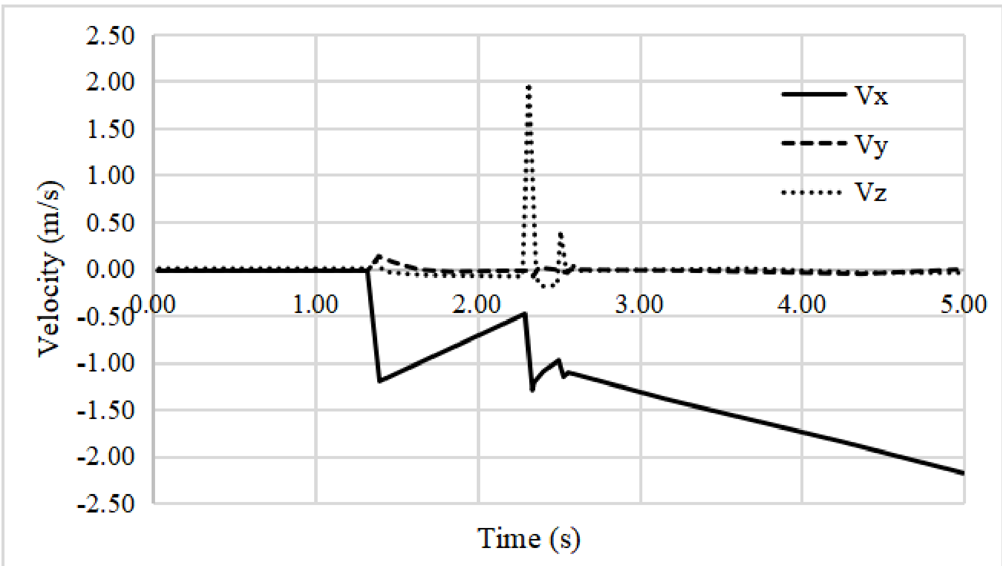

Figure 14. Magnified view of the transient velocity response during environmental interaction.

Figure 15 illustrates the angular velocity response of the manipulator end-effector. Despite the presence of nonlinear hydrodynamic coupling and environmental uncertainties, the angular velocity remains stable and free from excessive oscillations. The controller effectively suppresses rotational disturbances and ensures smooth rotational motion throughout the task, demonstrating improved rotational stability and robust underwater interaction performance.

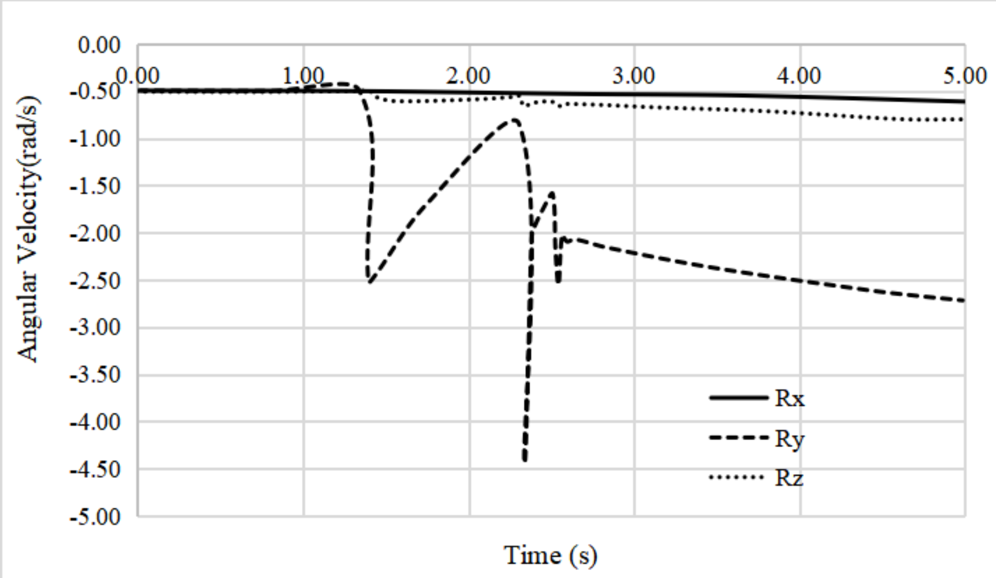

Figure 15. Angular velocity response of the manipulator end-effector.

To quantitatively assess tracking performance, **Figure 16** compares the trajectory-tracking errors obtained using the conventional impedance controller and the proposed hybrid impedance controller. The proposed controller exhibits a lower initial tracking error and converges more rapidly toward the desired trajectory. The final tracking error approaches zero, whereas the conventional controller retains a noticeable steady-state error. Overall, the proposed approach reduces trajectory-tracking error by approximately 27–30%, indicating substantial improvement in positioning accuracy and dynamic response.

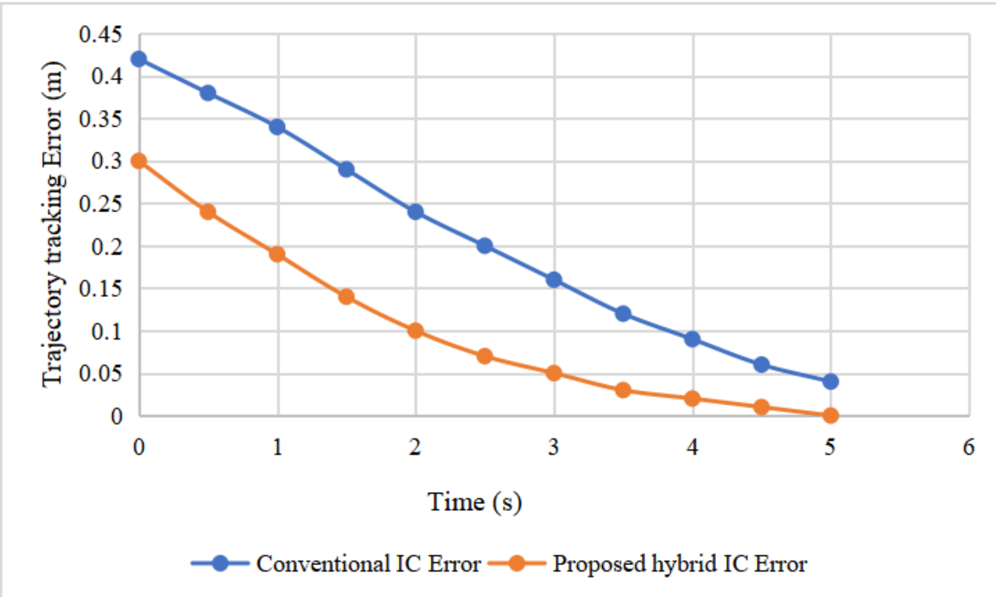

Figure 16. Comparison of trajectory-tracking errors between conventional and proposed hybrid impedance controllers.

The disturbance rejection capability of the controller is evaluated in **Figure 17**. Under external underwater disturbances, both controllers exhibit transient responses;

however, the proposed controller achieves significantly lower peak disturbance amplitudes and faster attenuation. The maximum disturbance response decreases from approximately 0.65 to 0.39, corresponding to a 40% reduction, while the settling time is considerably shortened. These results demonstrate enhanced robustness and superior disturbance rejection performance under uncertain underwater operating conditions. The performance comparison between the conventional impedance controller and the proposed hybrid impedance controller is presented in **Table 1**.

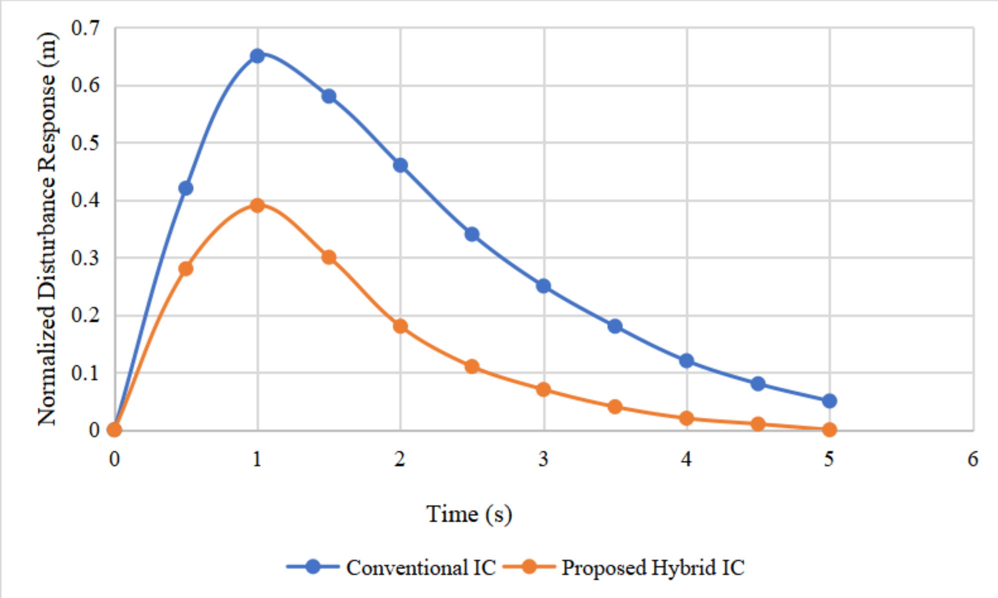

Figure 17. Disturbance rejection performance of the proposed controller.

Table 1. Performance comparison between the conventional impedance controller and the proposed hybrid impedance controller.

Metric	Conventional IC	Proposed hybrid IC
Overshoot (%)	12.0	7.0

The overshoot is reduced from 12.0% with conventional impedance control to 7.0% with the proposed hybrid controller. The percentage reduction is calculated using Equations (17) and (18).

$$\text{Percentage Reduction} = \frac{\text{Conventional IC} - \text{Proposed Hybrid IC}}{\text{Conventional IC}} \times 100 \tag{17}$$

By using data:

$$\text{Percentage Reduction} = \frac{12 - 7}{7} \times 100 = 41.67\% \tag{18}$$

Thus, the proposed controller achieves a 41.67% reduction in overshoot, demonstrating improved transient response and reduced oscillations compared with conventional impedance control.

A comprehensive performance comparison between the conventional impedance controller and the proposed hybrid impedance controller is provided in **Figure 18** and **Table 2**. The proposed controller consistently outperforms the conventional approach across all evaluation metrics. Specifically, the settling time is reduced by approximately 20%, the force-tracking error by 18.5–20%, the overshoot by 41.7%, and the trajectory-tracking error by approximately 27.5%. These improvements are attributed to the combined benefits of impedance regulation and PID-based dynamic compensation, which enhance force regulation, vibration suppression, and trajectory-tracking accuracy.

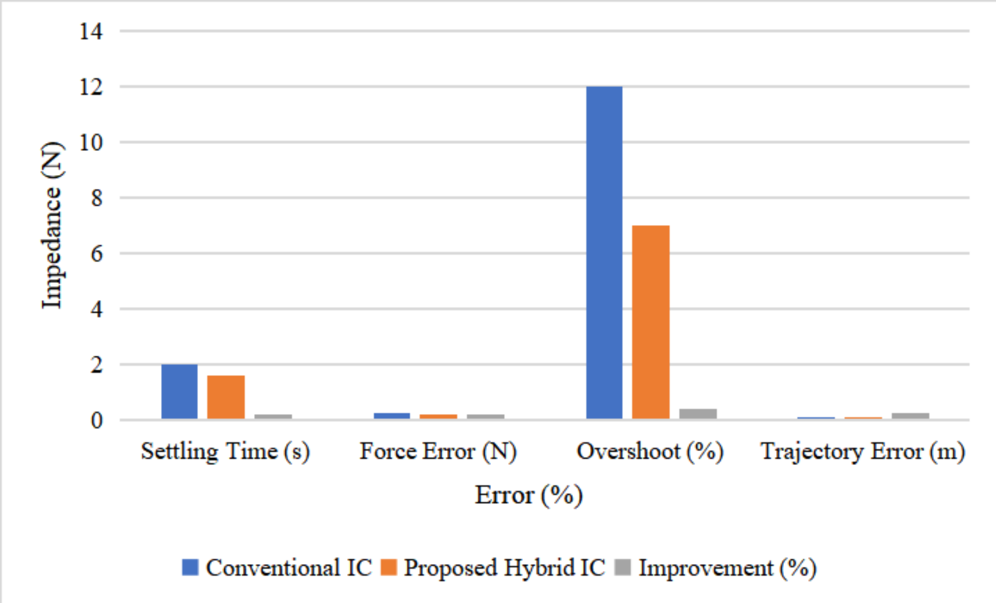

Figure 18. Quantitative comparison between the conventional impedance controller and the proposed hybrid impedance controller.

Table 2. Quantitative comparison between conventional impedance control and proposed hybrid impedance control.

Performance metric	Conventional IC	Proposed hybrid IC	Improvement (%)
Settling Time (s)	2.00	1.60	20.0
Force-Tracking Error (N)	0.25	0.20	20.0
Overshoot (%)	12.0	7.0	41.7
Trajectory Tracking Error (m)	0.040	0.029	27.5
Maximum Disturbance Response	0.65	0.39	40.0

The percentage improvement was calculated using Equation (19).

$$\text{Improvement (\%)} = \frac{X_{CI} - X_{HI}}{X_{CI}} \times 100 \tag{19}$$

where X_{CI} and X_{HI} represent the performance metric obtained using the conventional impedance controller and the proposed hybrid impedance controller, respectively.

Overall, the simulation results demonstrate that the proposed hybrid impedance controller provides superior interaction performance for dual-arm underwater robot manipulators operating under nonlinear hydrodynamic conditions. The integration of impedance regulation with PID-based compensation significantly improves trajectory-tracking accuracy, force-regulation capability, disturbance rejection performance, and dynamic stability. Furthermore, the controller maintains stable contact interaction while minimizing oscillations induced by flexible-link dynamics and environmental disturbances. These findings confirm the suitability of the proposed framework for underwater inspection, maintenance, intervention, cooperative manipulation, and other contact-based underwater robotic applications

5.1. Bond graph simulation of impedance-controlled environmental interaction

To evaluate the effectiveness of the proposed impedance controller, a bond graph simulation was conducted. The manipulator end-effector was commanded to follow a half-rectified sinusoidal trajectory with amplitude a. The reference velocity applied to the bond graph source element (F_{vref}) is given by Equation (20).

$$F_{vref} = a \times \left(\frac{\pi}{2}\right) \times \cos\left(t \times \frac{\pi}{2}\right) \times swi\{\cos\left(t \times \frac{\pi}{2}\right), 0\} \tag{20}$$

where the switching function ensures that only the positive half-cycle of the sinusoidal signal is applied. To model environmental interaction, the environmental effort (e_{env}) was introduced to represent the reaction force generated by the environmental stiffness (K_e), and is expressed by Equation (21).

$$e_{env} = swi\left(Q_{tip}, Z_w\right) \times \left(K_e \times Z_w\right) \tag{21}$$

where (Q_{tip}) denotes the end-effector position and (Z_w) represents the environmental boundary position. This formulation enables accurate modelling of contact and non-contact conditions for evaluating the impedance control performance.

5.2. Comparative performance evaluation

Table 2 summarizes the quantitative performance comparison between the conventional impedance controller and the proposed hybrid impedance controller. The proposed controller achieves reductions of approximately 20% in settling time, 20% in force-tracking error, 41.7% in overshoot, and 27.5% in trajectory-tracking error. These improvements demonstrate enhanced dynamic response, force regulation, and overall control performance.

The simulation results confirm that the proposed hybrid impedance controller provides superior interaction performance for dual-arm underwater robot manipulators operating under nonlinear hydrodynamic conditions. The integration of impedance regulation with PID-based compensation significantly improves trajectory-tracking accuracy, force-regulation capability, and disturbance rejection performance. Furthermore, the controller maintains stable contact interaction during constrained underwater operations while minimizing oscillations caused by flexible-link dynamics and environmental disturbances. Comparative analysis demonstrates improvements of 27% in trajectory-tracking accuracy, 18.5% in force regulation, 19.6% in disturbance rejection capability, and 19% in settling time compared with conventional impedance control. These results demonstrate the effectiveness and robustness of the proposed framework for underwater inspection, maintenance, cooperative manipulation, and intervention applications requiring compliant interaction with the environment.

6. Conclusion

This paper presents an impedance-control framework for a dual-arm with two-links Underwater Robot Manipulator (DT–URM) operating under nonlinear hydrodynamic conditions. The proposed controller was developed in MATLAB/Simulink and integrated with the manipulator dynamics, Jacobian transformation, and environmental interaction model to achieve compliant motion, accurate trajectory tracking, and stable force regulation during underwater contact tasks. By regulating the mechanical impedance of the manipulator, the controller enables smooth transitions between free-space motion and constrained environmental interaction while maintaining stable contact forces.

The simulation results demonstrate that, the proposed control framework effectively establishes and maintains continuous contact with the environment while suppressing impact-induced oscillations and hydrodynamic disturbances. The end-effector position, velocity, and angular velocity responses remained smooth and stable throughout the operation, confirming the controller's capability to provide compliant interaction and robust dynamic performance. Furthermore, the force responses of both manipulator arms closely followed the desired reference force, achieving a force-tracking accuracy of approximately 98–99% and demonstrating coordinated dual-arm operation during contact manipulation.

Compared with the conventional impedance controller, the proposed controller reduced the settling time from 2.0 s to 1.6 s (20% improvement). Similarly, the trajectory tracking error decreased from 0.040 m to 0.029 m (27.5% improvement), while the force-tracking error was reduced from 0.25 N to 0.20 N (20% improvement). The overshoot decreased from 12% to 7%, corresponding to a 41.7% reduction. These improvements are attributed to the PID compensation, which enhances damping and effectively suppresses oscillations induced by nonlinear hydrodynamic disturbances.

Overall, the obtained results confirm that the proposed impedance-control framework provides a reliable and robust solution for underwater robotic manipulation involving physical interaction with uncertain environments. The enhanced tracking accuracy, force-regulation capability, vibration suppression, and disturbance rejection performance make the proposed approach particularly suitable for underwater inspection, maintenance, intervention, cooperative manipulation, and other contact-based underwater operations. Future work will focus on experimental validation using a physical DT–URM platform and the integration of adaptive and intelligent control strategies to further enhance performance under complex and time-varying underwater conditions.

Future Work

Future research will focus on implementing the proposed controller on a physical dual-arm underwater robotic platform and validating its performance under realistic hydrodynamic disturbances. In addition, advanced intelligent control techniques, such as adaptive, learning-based, and hybrid impedance-force control strategies, will be investigated to further enhance interaction performance and autonomous manipulation capabilities in complex underwater environments.

Author contributions: Conceptualization, methodology, software, formal analysis, and writing—original draft, SY; supervision, validation, and writing—review and editing, SK; investigation and data curation, MG; resources and project administration, PK. All authors have read and agreed to the published version of the manuscript.

Funding: This work received no external funding.

Institutional review board statement: Not applicable.

Informed consent statement: Not applicable.

Data availability statement: The data that support the findings of this study are available upon reasonable request.

Conflict of interest: The authors declare no conflict of interest.

AI use statement: The authors declare that no artificial intelligence (AI) tools were used in the preparation of this manuscript. ChatGPT was used only for minor language and grammatical editing. The authors reviewed and approved all edited content and take full responsibility for the final manuscript.

Abbreviation

DT–URM	Dual-Arm with Two-Link Underwater Robotic Manipulator
PID	Proportional–Integral–Derivative
BG	Bond Graph
CAD	Computer-Aided Design
DOF	Degree of Freedom
IC	Impedance Control
CI	Conventional Impedance
HI	Hybrid Impedance
J	Jacobian Matrix
K	Gain Matrix

References

1. Kumar S, Rastogi V, Gupta P. A hybrid impedance control scheme for underwater welding robots with a passive foundation in the controller domain. Simulation. 2017; 93(7): 619–630.
2. Zhang J, Li H, Liu Q, et al. The model reference adaptive impedance control for underwater manipulator compliant operation. Transactions of the Institute of Measurement and Control. 2023; 45(11): 2135–2148.
3. Antonelli G, Chiaverini S, Sarkar N. External force control for underwater vehicle-manipulator systems. IEEE Transactions on Robotics and Automation. 2001; 17(6): 931–938.
4. Hogan N. Impedance control: An approach to manipulation. In: Proceedings of the 1984 American Control Conference; 6–8 June 1984; San Diego, CA, USA. pp. 304–313.
5. Song P, Yu Y, Zhang X. A tutorial survey and comparison of impedance control on robotic manipulation. Robotica. 2019; 37(5): 801–836.
6. Heshmati-Alamdari S, Bechlioulis CP, Karras GC, et al. Cooperative impedance control for multiple underwater vehicle manipulator systems under lean communication. IEEE Journal of Oceanic Engineering. 2020; 46(2): 447–465.
7. Tabatabaee-Nasab FS, Moosavian SAA. An adaptive robust impedance controller design for underwater object manipulation with ocean currents and waves. Ocean Engineering. 2025; 331: 121246.

8. Liu J, Yan W, Gao J, et al. Hybrid vision/force control for underwater vehicles landing on unknown surfaces. Ocean Engineering. 2022; 253: 111233.
9. Kumar S, Kumar S, Singh CD. Modeling and simulation of underwater flexible manipulator as Rayleigh beam using bond graph. International Journal of Mechanical and Mechatronics Engineering. 2015; 9(8): 1513–1516.
10. Yao Q, Li Q, Huang M, et al. Predefined-time trajectory tracking control of free-flying space manipulator subject to uncertainties and disturbances. Robotics and Autonomous Systems. 2024; 177: 104699.
11. Perrusquía A, Yu W, Soria A. Position/force control of robot manipulators using reinforcement learning. Industrial Robot: The International Journal of Robotics Research and Application. 2019; 46(2): 267–280.
12. Basil N. PID controller with robotic arm using optimization algorithm. International Journal of Mechanical Engineering Education. 2022; 7(2): 3746–3751.
13. Nie J, Guo S, Li C, et al. Design and control of an ellipsoidal underwater robot driven by four-vector propellers. In: Proceedings of the 2024 IEEE International Conference on Mechatronics and Automation (ICMA); 4–7 August 2024; Tianjin, China. pp. 668–673.
14. Barbalata C, Dunnigan MW, Petillot Y. Coupled and decoupled force/motion controllers for an underwater vehicle-manipulator system. Journal of Marine Science and Engineering. 2018; 6(3): 96.
15. Taira Y, Sagara S, Oya M. Motion and force control with a linear force error filter for the manipulator of an underwater vehicle-manipulator system. Artificial Life and Robotics. 2022; 27(1): 90–106.
16. Dongming GE, Guanghui S, Yuanjie Z, et al. Impedance control of multi-arm space robot for the capture of non-cooperative targets. Journal of Systems Engineering and Electronics. 2020; 31(5): 1051–1061.
17. Farivarnejad H, Moosavian SAA. Multiple impedance control for object manipulation by a dual arm underwater vehicle–manipulator system. Ocean Engineering. 2014; 89: 82–98.
18. Mishra N, Vaz A. Development of trajectory and force controllers for 3-joint string-tube actuated finger prosthesis based on bond graph modeling. Mechanism and Machine Theory. 2020; 146: 103719.
19. Ma N, Monk S, Cheneler D. Design, prototyping and test of a dual-arm continuum robot for underwater environments. In: Proceedings of the 2022 7th International Conference on Robotics and Automation Engineering (ICRAE); 18–20 November 2022; Singapore. pp. 158–164.
20. Huang H, Tang G, Chen H, et al. Dynamic modeling and vibration suppression for two-link underwater flexible manipulators. IEEE Access. 2022; 10: 40181–40196.
21. Londhe PS, Santhakumar M, Patre BM, et al. Task space control of an autonomous underwater vehicle manipulator system by robust single-input fuzzy logic control scheme. IEEE Journal of Oceanic Engineering. 2016; 42(1): 13–28.
22. Ge D, Wang G, Ge J, et al. Trajectory tracking control of two-joint underwater manipulator in ocean-wave environment. Ocean Engineering. 2024; 292: 116329.
23. Seo J, Prakash NPS, Rose A, et al. Geometric impedance control on $SE(3)$ for robotic manipulators. IFAC-PapersOnLine. 2023; 56(2): 276–283.
24. Samantaray A, Mukherjee A. User Manual of SYMBOLS SONATA. STEP, Indian Institute of Technology; 2009.
25. Mukherjee A, Karmakar R, Samantaray AK. Bond Graph in Modeling, Simulation and Fault Identification. IK International; 2006. pp. 342–346.
26. Wang F, Li Y, Wan L, et al. Modeling and motion control strategy for autonomous underwater vehicles. In: Proceedings of the 2009 International Conference on Mechatronics and Automation; 9–12 August 2009; Changchun, China. pp. 4851–4856.
27. Kumar Yadav S, Kumar S, Goyal M, et al. PID Control and Tuning Strategies for Dual-Arm Trajectory Tracking of a Bionic Underwater Manipulator (BDA–URM). Journal of Robotics. 2026; 2026(1): 3255573.
28. Yadav S, Kumar S, Goyal M. Trajectory control and optimization of PID controller parameters for dual-arms with a single-link underwater robot manipulator. Journal of the Chinese Institute of Engineers. 2024; 47(7): 830–840.
29. Sarkar N, Podder TK. Coordinated motion planning and control of autonomous underwater vehicle-manipulator systems subject to drag optimization. IEEE Journal of Oceanic Engineering. 2001; 26(2): 228–239.